Investigation on the Distribution of Fluorine and Boron in Polycrystalline Silicon/Silicon Systems

T. P. Chen, T. F. Lei, and C. Y. Chang

Department of Electronics Engineering and Institute of Electronics, National Chiao Tung University, and National Nano Device Laboratory, Hsinchu, Taiwan

W. Y. Hsieh and L. J. Chen

Department of Materials Science and Engineering, National Tsing Hua University, Hsinchu, Taiwan

ABSTRACT

The behaviors of fluorine in BF_2^+ implanted polycrystalline silicon (poly-Si) on silicon have been investigated in the annealing temperature range of 850 to 1100°C. The distribution of fluorine atoms as functions of temperature and time have been monitored by the secondary ion mass spectroscopy (SIMS) and cross-sectional transmission electron microscopy (XTEM). The XTEM micrographs revealed that fluorine bubbles are distributed in the poly-Si and at the original poly-Si/Si interface after annealing. The locations of bubbles were found to correspond to the fluorine peaks in the SIMS depth-concentration profiles. The presence of the boron peak at the original poly-Si/Si interface is attributed to the gettering of boron atoms by the fluorine bubbles. Moreover, the boron profiles in the silicon substrates are sensitive to thermal budget due to the pileup of fluorine atoms at the poly-Si/Si interface. The pileup of fluorine at the poly-Si/Si interface leads to an enhancement of epitaxial regrowth of poly-Si films and the formation of fluorine bubbles. Consequently, higher surface dopant concentration and deeper junction depth were obtained.

Introduction

A heavily doped polycrystalline silicon (poly-Si) as a diffusion source to form shallow junctions and device contacts has been widely used in complementary metal-oxide semiconductor (CMOS) devices and poly-Si emitter bipolar transistors.[1,2] The advantages of heavily doped poly-Si films as diffusion source are increasing packing density, switching speed, improvement of dc current gain, and elimination of aluminum spiking through p-n shallow junction.[1-4] The physical structure and the electrical characteristics of poly-Si/Si interface have been widely studied. It is well known that the morphology of poly-Si/Si interface plays an important role in shaping the diffusion profiles of doping impurity and the electrical properties of CMOS devices and poly-Si emitter bipolar transistors.[5-9]

Because complementary bipolar CMOS (BiCMOS) circuits have advantages for both digital and analog application, it is important to study p^+ poly-Si films as a diffusion source for the fabrication of vertical p-n-p polysilicon bipolar transistors.[6,9-10] The heavily doped p^+ polysilicon films are often doped by the BF_2^+ implantation.[6,10] During BF_2^+ implantation, fluorine atoms are also incorporated into poly-Si films. The effects of fluorine on the p^+ poly-Si gate devices have been widely investigated.[11,12] It is well known that the presence of fluorine atoms enhance boron penetration through thin gate oxide into silicon substrate. However, the roles of fluorine in the poly-Si/Si systems are much less investigated. Recently, it was found that the epitaxial growth of poly-Si films was apparently promoted by the breakup of native oxides at the poly-Si/Si interface in the presence of fluorine atoms.[13,14] However, the exact nature of fluorine in the poly-Si/Si systems as functions of annealing temperature and time has not been systematically studied. In this paper, the distribution and the roles of fluorine in the poly-Si/Si as functions of annealing temperature and time were examined by cross-sectional transmission electron microscopy (XTEM) and secondary ion mass spectroscopy (SIMS). It was observed that fluorine bubbles are distributed in the as-implanted fluorine peak region and at the original poly-Si/Si interface. The effects of fluorine on the boron diffusion profiles and the structure morphology of poly-Si/Si were also studied. As compared with the Si-B layer source,[15] the higher surface boron concentration, C_s, and a deeper junction depth for BF_2^+ implanted poly-Si source are considered to be the fluorine effects. The surface boron concentration, C_s, value can be obtained by

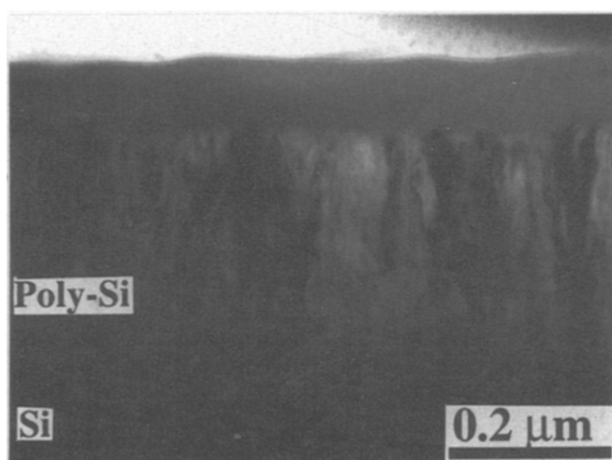

Fig. 1. XTEM micrograph of the BF_2^+ as-implanted poly-Si/Si with an energy of 80 keV and a dose of 6×10^{15} cm^{-2}.

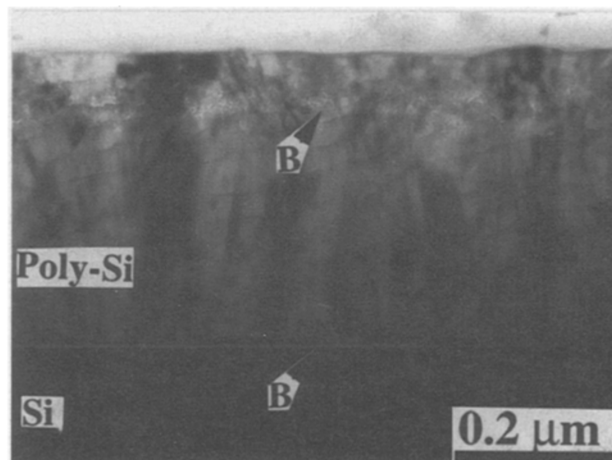

Fig. 2. XTEM micrograph of BF_2^+ implanted poly-Si/Si after thermal annealing at 850°C for 30 min. B represents the bubbles.

Downloaded on 2014-04-28 to IP 140.113.38.11 address. Redistribution subject to ECS terms of use (see ecsdl.org/site/terms_use) unless CC License in place (see abstract).

the linear extrapolation of boron profiles in the silicon toward the poly-Si/Si interface.[16,17]

Experimental

The substrates used in this experiment were n-type, (001)Si wafers with a resistivity of 0.5 to 2 Ω-cm. Prior to poly-Si film deposition, all wafers were dipped in a dilute HF solution to remove the surface native oxide followed by a deionized water rinse. Then, poly-Si films with a thickness of 350 nm were deposited in a low pressure chemical vapor deposition (LPCVD) system at 625°C with SiH_4 gas. The deposition pressure and deposition rate were about 180 to 220 mTorr and 11 nm/min, respectively. During the LPCVD poly-Si deposition process, a native oxide was formed at the poly-Si/Si interface. All wafers were then implanted with 80 keV BF_2^+ to a dose of 6×10^{15} cm^{-2}. After implantation, the wafers were annealed in the temperature range of 850 to 1100°C. The structures of poly-Si/Si were examined by XTEM using a JEOL 200 CX microscope, operating at 200 keV. The boron and fluorine distribution profiles was obtained with a Cameca IMS-4f ion microanalyzer using O_2^+ primary ion bombardment.

Results and Discussion

XTEM examination of poly-Si/Si samples.—As-implanted poly-Si/Si samples.—Figure 1 shows an XTEM micrograph of a BF_2^+-implanted poly-Si/Si sample. It can be seen that the poly-Si surface layer was completely amorphized by the BF_2^+ implantation to a depth of about 100 nm from the surface.

850°C annealed samples.—Figure 2 shows the XTEM micrograph of BF_2^+-implanted poly-Si/Si after annealing at 850°C for 30 min. It has been assumed that the fluorine is immobile within the grains and that there is a strong emission of fluorine from the grains into the grain boundaries.[12] However, the nature of fluorine in the poly-Si is not clearly understood owing to the complicated structure of poly-Si. As shown in Fig. 2, it can be seen that the amorphous layer was recrystallized into poly-Si after annealing. The recrystallized poly-Si films consists of residual defects. A high density of small fluorine bubbles was distributed in the recrystallized poly-Si films. The bubbles in the poly-Si films are distributed in a depth range of 60 to 110 nm beneath the poly-Si surface, which is near the original a-Si/poly-Si surface. The distribution of bubbles is consistent with the observation of the presence of a fluorine peak in the recrystallized poly-Si films after annealing. It has been reported that the fluorine atoms tend to be gettered in the residual damage region.[18] Fluorine bubbles are apparently formed from the accumulation of fluorine atoms and vacancies since the solid solubility of fluorine atoms is rather low. The fluorine bubbles were also observed in high dose BF_2^+-implanted silicon after annealing at 1000 to 1100°C.[19,20] However, the formation of fluorine bubbles in the poly-Si film had not been reported previously. As shown in Fig. 2, the epitaxial alignment of poly-Si films did not occur in the 850°C annealed sample. It should be noted that a thin uniform layer of bubbles was found to develop at the original poly-Si/Si interface. The thickness of this bubble layer was estimated to be about 2.5 nm. The results are consistent with the SIMS fluorine profile which shows a high concentration of fluorine atoms accumulated at the poly-Si/Si interface after annealing. It has been reported that the fluorine atoms could react with native oxide and Si to form Si oxyfluoride and Si fluoride.[21] Hence, the fluorine atoms accumulated at the poly-Si/Si interface may react with interfacial native oxide and form fluorine bubbles. As mentioned previously, the morphology of poly-Si/Si interface plays an important role in shaping the diffusion profiles of doping impurity and the electrical properties of poly-Si emitter bipolar transistors. However, the formation of fluorine bubbles at the poly-Si/Si interface has not been reported previously.

900°C annealed samples.—Figures 3a and b show XTEM micrographs of samples after annealing at 900°C for 30 and 60 min, respectively. The bubbles are also distributed in the recrystallized poly-Si films for both samples. The distribution of bubbles in the poly-Si/Si is similar to that of 850°C annealed samples. The bubbles in the recrystallized poly-Si films were found to grow larger as compared with those in 850°C annealed samples. The sizes of bubbles were measured to be 3 to 20 nm. The XTEM micrographs also reveal that the poly-Si films were epitaxially aligned with silicon substrate in 900°C annealed samples. The maximum thickness of the epitaxially aligned poly-Si films were estimated to be 30 and 70 nm for 30 and 60 min annealed samples, respectively. In contrast, a partial epitaxial regrowth of poly-Si on Si was observed in the poly-Si/Si with a thin Si-B layer as diffusion source after annealing at 1000°C for 30 min.[15] Moreover, the partial epitaxial regrowth of poly-Si on Si was observed in the unimplanted poly-Si/Si after annealing at 1100°C for 30 min. On the other hand, the epitaxial growth of poly-Si on Si was promoted by the presence of fluorine atoms at the poly-Si/Si interface. It should be noted that the fluorine bubbles were also observed at the original poly-Si/Si interface after epitaxial regrowth of poly-Si on Si. The layer of bubbles located at the poly-Si and Si interface was disrupted to form bands of

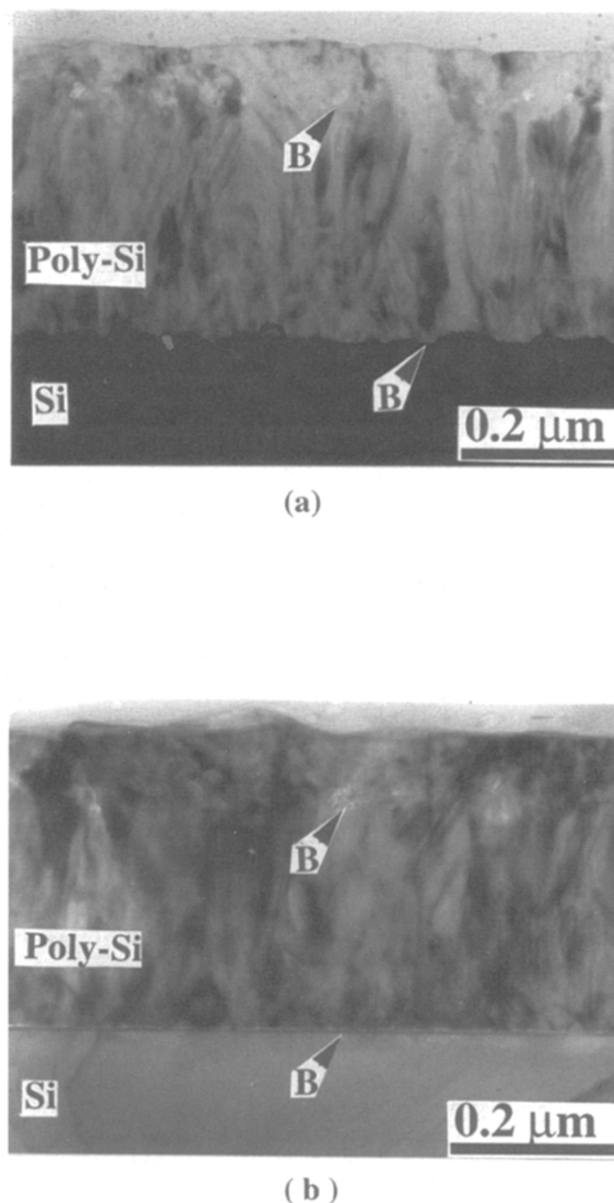

Fig. 3. XTEM micrographs of BF_2^+ implanted poly-Si/Si after thermal annealing at 900°C for (a) 30 and (b) 60 min. B represents the bubbles.

Downloaded on 2014-04-28 to IP 140.113.38.11 address. Redistribution subject to ECS terms of use (see ecsdl.org/site/terms_use) unless CC License in place (see abstract).

bubbles during the epitaxial growth of poly-Si films. The thickness and length of bubble bands were estimated to be 3.5 and 180 nm and 5 and 135 nm for 30 and 60 annealed samples, respectively.

950°C annealed samples.—Figures 4a, b, and c show the XTEM micrograph of samples after annealing at 950°C for 15, 30, and 60 min, respectively. It can be seen that most of the bubbles in the recrystallized poly-Si films are distributed in a depth range of 60 to 110 nm beneath the poly-Si surface. The size of bubbles in the recrystallized poly-Si films was found to be larger as compared with those of 900°C annealed samples. The maximum size of bubbles in the poly-Si film in 950°C annealed samples is as large as 40 nm. However, the density of bubbles in poly-Si film was decreased with annealing temperature and time. The XTEM micrographs reveal that approximately 20, 30, and 45% of poly-Si films were epitaxially aligned with the silicon substrate in samples annealed for 15, 30, and 60 min, respectively. The roughness of the epitaxial regrowth front of poly-Si film is increased with annealing time. In addition, the fluorine bubbles were also found to be present at the original poly-Si/Si interface in samples annealed at 950°C. The shape of bubbles at the original poly-Si/Si interface is similar to that in 900°C annealed samples for annealing time less than 30 min. However, the length and width of bubble bands were decreased and increased with annealing time, respectively. For a 60 min annealed sample, the shape of bubbles at the poly-Si/Si interface were observed to be truncated octahedra with truncated faces parallel to {100}. It is interesting to note that one of the prominent truncated faces of the bubbles is the original poly-Si/Si interface. The maximum size of the bubble is as large as 24 nm.

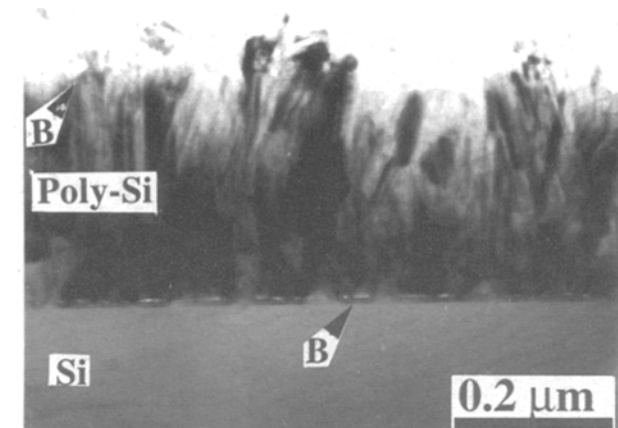

(a)

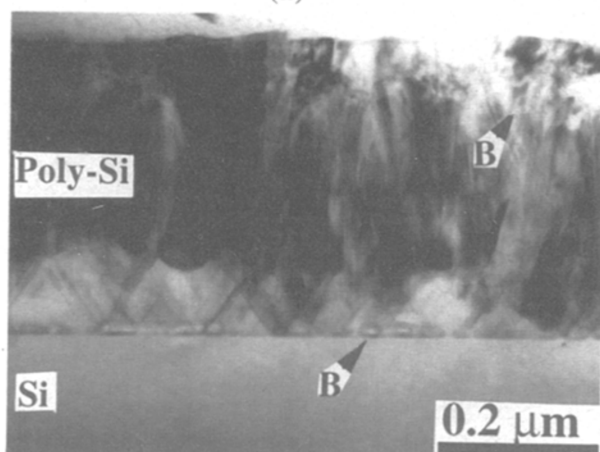

(b)

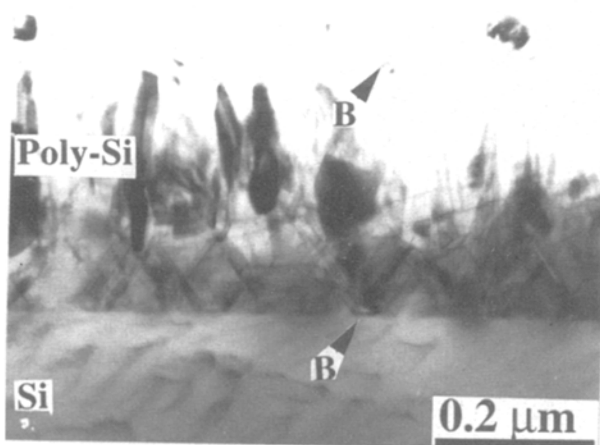

(c)

Fig. 4. XTEM micrographs of BF_2^+ implanted poly-Si/Si after thermal annealing at 950°C for (a) 15, (b) 30, and (c) 60 min. B represents the bubbles.

1000°C annealed samples.—Figures 5a, b, and c show the XTEM micrographs of samples annealed at 1000°C for 5, 30, and 60 min, respectively. Bubbles were also observed in the recrystallized poly-Si films. However, the average size of bubbles in the poly-Si films in 1000°C annealed sample was smaller than that of 950°C annealed samples. The sizes of bubble were estimated to be 10 to 30 nm. In addition, the density of bubbles in the poly-Si film is lower than those in 850 to 950°C annealed sample. The XTEM micrographs reveal that approximately 15, 45, and 60% of poly-Si films were aligned epitaxially to silicon in sample annealed for 5, 30, and 60 min, respectively. The roughness of epitaxial regrowth front was found to increase with annealing temperature or time. Moreover, a high density of twins was observed to be distributed in the epitaxial regrowth films. The bubbles were also observed at the poly-Si/Si interfaces in all three samples. The shape of bubbles at the poly-Si/Si interface were observed to be truncated octahedra with truncated faces parallel to {100}. One of truncated faces of bubbles correspond to the original poly-Si/Si interface. It was also found that the average size and the density of bubbles at the original poly-Si/Si interface were increased and decreased with annealing time, respectively. The maximum size of bubbles at the poly-Si/Si interface could be as large as 65 nm (1000°C, 60 min).

1100°C annealed samples.—Figures 6a, b, and c show the XTEM micrographs of BF_2^+-implanted poly-Si/Si after annealing at 1100°C for 5, 15, and 30 min, respectively. It is seen that most of poly-Si films are epitaxially aligned with the silicon substrate for all three samples. A high density of twins were also observed to be distributed in the epitaxial regrowth poly-Si films. Two groups of fluorine bubbles were observed in epitaxial regrowth films. The depth distribution of bubbles is the same as those in the samples annealed at 850 to 1000°C. Some of the bubbles were observed in depths ranging from 50 to 100 nm beneath the surface. However, the size and the density of bubbles in the as-implanted peak regions are much smaller than those in 900 to 1000°C annealed samples. The size of bubble was estimated to be 5 to 25 nm. Another group of bubbles was distributed at the original poly-Si/Si interface. The shape of bubbles at the original poly-Si/Si interface is the same as that in the 1000°C annealed samples. It was also found that the number of bubbles at the poly-Si/Si interface decreased with increasing annealing time; however, the size of the bubbles did not increase with annealing time. This implies that some of fluorine atoms outdiffused from the poly-Si/Si interface for 1100°C annealed sample. The re-

Downloaded on 2014-04-28 to IP 140.113.38.11 address. Redistribution subject to ECS terms of use (see ecsdl.org/site/terms_use) unless CC License in place (see abstract).

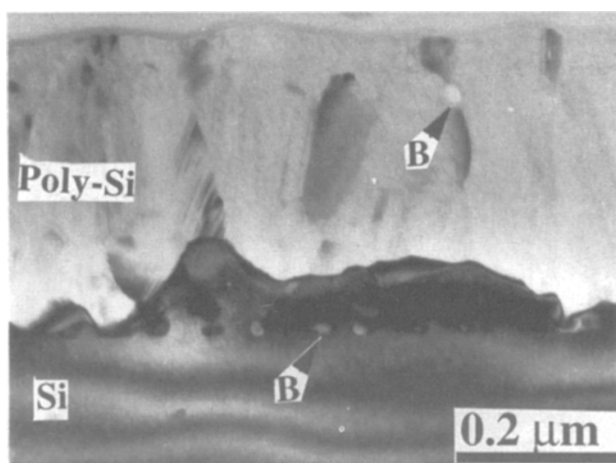

(a)

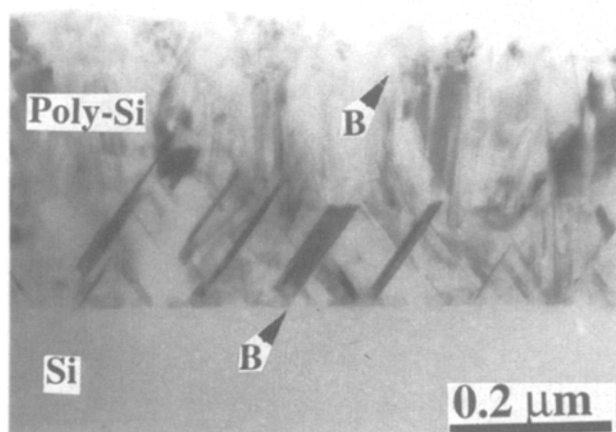

(b)

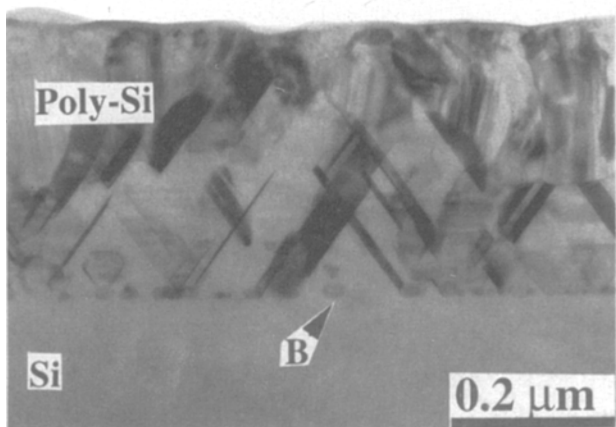

(c)

Fig. 5. XTEM micrograph of BF_2^+ implanted poly-Si/Si after thermal annealing at 1000°C for (a) 10, (b) 30, and (c) 60 min. B represents the bubbles.

sults are consistent with the SIMS fluorine profile which shows the fluorine concentrations in the as-implanted peak region and at the poly-Si/Si interface are considerably decreased in 1100°C annealed sample.

Finally, the variations of the shape and the size of the fluorine bubbles and the epitaxial regrowth of poly-Si on the substrate with annealing temperatures and times are summarized in Table I.

SIMS fluorine profile.—Figure 7 shows the SIMS fluorine distribution profiles of BF_2^+ as-implanted poly-Si/Si and samples after thermal annealing in the temperature range of 850 to 1100°C for 30 min. The as-implanted fluorine peak is present at a depth of 75 nm beneath the poly-Si surface. After thermal annealing, the fluorine atoms are redistributed significantly and double fluorine peaks are

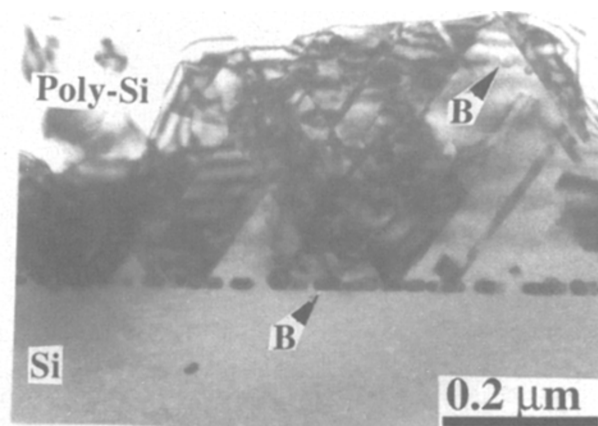

(a)

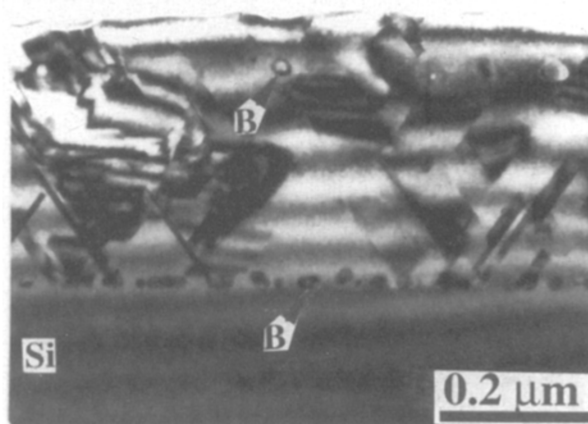

(b)

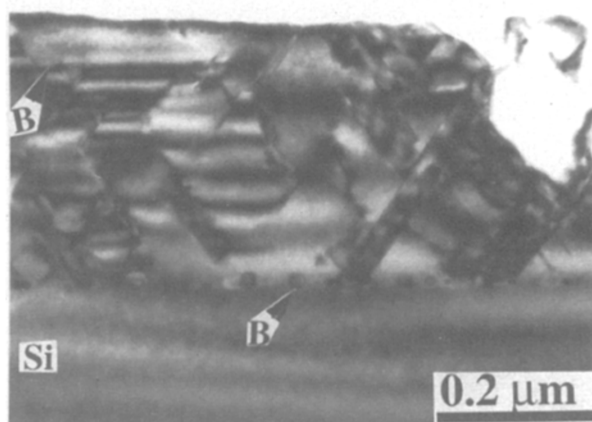

(c)

Fig. 6. XTEM micrographs of BF_2^+ implanted poly-Si/Si after thermal annealing at 1100°C for (a) 5, (b) 15, and (c) 30 min. B represents the bubbles.

Downloaded on 2014-04-28 to IP 140.113.38.11 address. Redistribution subject to ECS terms of use (see ecsdl.org/site/terms_use) unless CC License in place (see abstract).

Table I. The variations of the shape and the size of fluorine bubble and the epitaxial regrowth of poly-Si with annealing temperatures and times.

Samples (°C/min)	Shape of bubble at the poly-Si/Si interface (nm)	Size of bubble at the poly-Si/Si interface (nm)	Size of bubble in as-implanted F peak regions (nm)	Epitaxial regrowth of poly-Si (%)
850/30	Bubble layer	2.5	2 ~ 8	No
900/30	Bubble band	(3.5, 180)	3 ~ 20	Partly, 5
900/60	Bubble band	(5, 135)	5 ~ 20	12.5
950/15	Bubble band	(7, 96)	10 ~ 40	20
950/30	Bubble band	(10, 90)	15 ~ 33	30
950/45	Bubble band, Truncated octahedra	(14, 60), 20	15 ~ 30	35
950/60	Truncated octahedra	6 ~ 24	10 ~ 33	45
1000/5	Truncated octahedra	6 ~ 33	10 ~ 30	14
1000/10	Truncated octahedra	10 ~ 36	10 ~ 36	22
1000/20	Truncated octahedra	10 ~ 50	10 ~ 40	35
1000/30	Truncated octahedra	10 ~ 55	10 ~ 43	45
1000/45	Truncated octahedra	6 ~ 60	13 ~ 30	52
1000/60	Truncated octahedra	10 ~ 65	10 ~ 20	60
1050/15	Truncated octahedra	10 ~ 40	6 ~ 20	65
1050/30	Truncated octahedra	14 ~ 50	6 ~ 20	88
1100/5	Truncated octahedra	10 ~ 50	8 ~ 18	80
1100/15	Truncated octahedra	10 ~ 45	9 ~ 25	90
1100/30	Truncated octahedra	10 ~ 40	8 ~ 15	96

observed in the SIMS fluorine profiles. The locations of fluorine peaks are consistent with the distribution of fluorine bubbles. A fluorine peak remains after thermal annealing at the as-implanted fluorine peak regions. The fluorine peak becomes narrower and weaker as the annealing temperature increases, except for the 900°C annealed sample. It is attributed to the outdiffusion of fluorine atoms and the formation of fluorine bubbles during thermal annealing. For the 900°C annealed sample, the fluorine profile becomes narrower as compared with the as-implanted profile; however, the fluorine peak concentration is greater than that of the as-implanted fluorine peak concentration. The phenomenon was also observed in heavily BF_2^+-implanted silicon after annealing at 900°C.[18] It is considered to be the gettering of fluorine atoms by the residual defects induced by the implantation. The gettering of fluorine atoms is relatively strong at this temperature. This is consistent with the XTEM observation, as shown in Fig. 3, that fluorine bubbles grew at this temperature. In addition, a fluorine peak was found to develop at the original poly-Si/Si interface after thermal annealing. As mentioned previously, a native oxide was formed at the poly-Si/Si interface during the LPCVD processes. It is well known that the oxide layer acts as a favorable site for the gettering of fluorine atoms.[20] Moreover, it has been reported that the diffusion of fluorine in the poly-Si films is dominated by the grain boundary diffusion.[12] Therefore, the fluorine peak at the poly-Si/Si interface arises from the diffusion of fluorine atoms along the poly-Si grain boundary and accumulates at the poly-Si/Si interface during thermal annealing. It should be noted that the fluorine peak concentration at the poly-Si/Si interface for 900°C annealed sample is also greater than those in other samples. However, the fluorine profiles at the poly-Si/Si interface are almost the same for 850, 950, and 1000°C samples. The reasons for this phenomenon are possibly the same as previously discussed. In samples annealed at 1100°C, both fluorine peaks are obviously decreased since most of the fluorine atoms diffused out. The results are consistent with those shown in Fig. 6 which indicates that the density and the size of bubbles in 1100°C samples are much smaller than those in 900 to 1000°C annealed samples. Between two fluorine peaks (the region −0.2 to 0.1 μm), the fluorine concentrations decreased with increasing annealing temperatures. It is considered to be the reduction of the grain boundary area because of the increasing of poly-Si grain size and the epitaxial regrowth of poly-Si films. Figures 8a and b show the SIMS fluorine profiles as a function of annealing time for 950 and 1000°C annealed samples, respectively. At the as-implanted fluorine peak region, the fluorine peaks become slightly narrower and lower as the annealing time increases. It is also considered to be due to the outdiffusion of fluorine atoms. However, the fluorine profiles at the poly-Si/Si interface are almost the same for different annealing times at temperatures 900 to 1000°C. The results indicate that the pileup of fluorine atoms at the poly-Si/Si interface is rapidly saturated. Moreover, the fluorine concentration is low in the region between two fluorine peaks. This indicates that the solid solubility of fluorine atoms in the poly-Si is rather low.

Boron diffusion profiles.—The diffusion behaviors of boron in the BF_2^+-implanted poly-Si/Si has been widely investigated by several researchers. However, the effects of fluorine on boron diffusion are not clearly understood. Figure 9 shows the boron profiles of as-implanted poly-Si/Si and samples after annealing in the temperature range of 850 to 1000°C for 30 min. It can be seen that a boron peak remains near the poly-Si surface for 850°C annealed samples. The boron peaks gradually disappeared as the annealing temperature increased. It has been reported that the diffusion of boron in the poly-Si is strongly affected by the solid solubility limit.[5,6] The boron diffusivity is drastically reduced in the poly-Si where the boron concentration exceeds the solid solubility limit. The formation of boron precipitates which reduces the boron diffusivity has been suggested for high dose BF_2^+-implanted samples.[6] In the present experiment, the XTEM micrographs reveal that the fluorine bubbles are distributed in the recrystallized poly-Si films after annealing. Moreover, the peak portions of F profiles are close to those of the B profiles. It has been reported that the dopant atoms are prone to be gettered by the residual defects. This indicated that the boron atoms could be gettered by the fluorine bubbles in the recrystallized poly-Si films.[23] In addition, it is interesting to note that a small boron peak is present at the poly-Si/Si interface in all annealed samples. The boron peak concentrations were estimated to be 1.7×10^{20}, 2.8×10^{20}, 2.6×10^{20}, and 2.7×10^{20} for 850, 900, 950, and 1000°C annealed sample, respectively. Moreover, as shown in Fig. 10a and b, it was found that the boron peak concentration are independent of annealing time for 950 and 1000°C annealed samples. The results are consistent with the fluorine profiles shown in Fig. 7 and 8. As shown previously, the fluorine bubbles were found to be present at the poly-Si/Si interface in all annealed samples. Therefore, the boron peak at the poly-Si/Si interface is considered to result from the gettering of boron atoms by the fluorine bubbles at the original poly-Si/Si interface.

It is well known that the segregation of the fluorine atoms in thin gate oxide enhances the penetration of boron atoms. As shown in Fig. 7, it can be seen that a large number of fluorine atoms piled up at the original poly-Si/Si interface after annealing. In a previous study, it was demonstrated that the boron profiles of BF_2^+-implanted

Downloaded on 2014-04-28 to IP 140.113.38.11 address. Redistribution subject to ECS terms of use (see ecsdl.org/site/terms_use) unless CC License in place (see abstract).

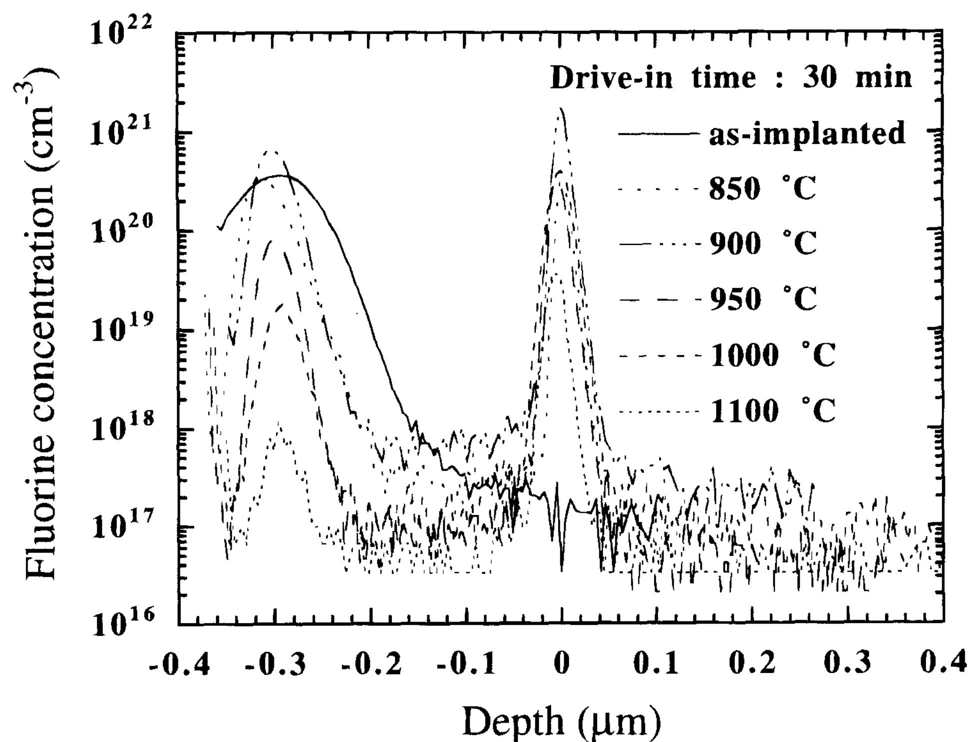

Fig. 7. SIMS fluorine distribution profiles of BF_2^+ as-implanted poly-Si/Si and samples after annealing at 850, 900, 950, 1000, and 1100°C for 30 min.

poly-Si source in the silicon substrates are more sensitive to the thermal budget than that of the Si-B layer source.[15] It is attributed to the larger surface concentration, C_s, for

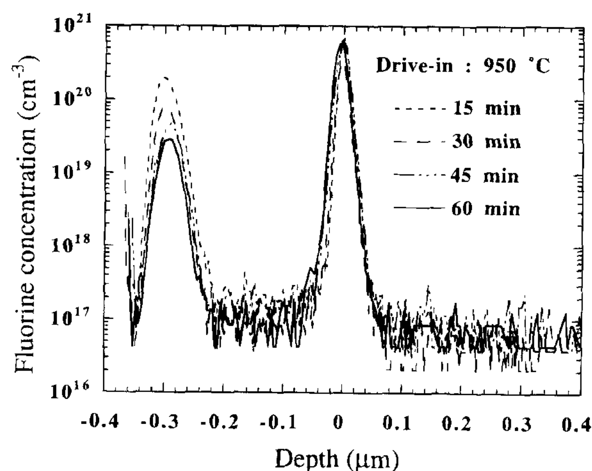

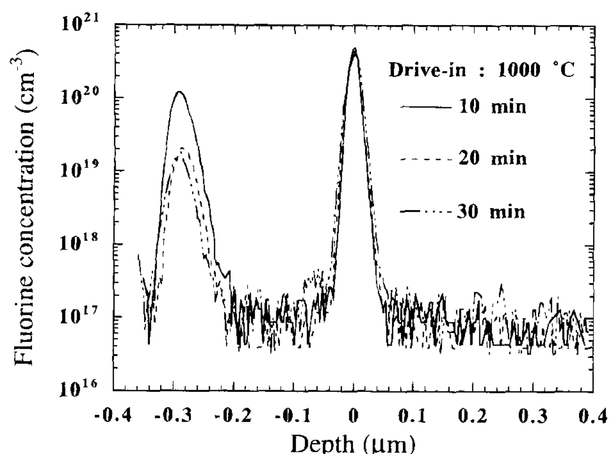

Fig. 8. SIMS fluorine distribution profiles of BF_2^+ implanted poly-Si/Si after thermal annealing at (a, top) 950 and (b, bottom) 1000°C for 10 to 60 min.

BF_2^+-implanted poly-Si/Si. As shown in Fig. 9, it can be seen that the C_s values increased with temperature. Moreover, the C_s values are independent of annealing time as seen from Fig. 10a and b. Therefore, the higher C_s values for BF_2^+-implanted poly-Si/Si are related to the presence of fluorine atoms. As discussed previously, the pileup of fluorine atoms at the poly-Si/Si interface enhances the epitaxial regrowth of poly-Si films and the formation of fluorine bubbles at the poly-Si/Si interface. The presence of fluorine atoms, in turn, leads to the higher C_s values and a deeper junction depth for BF_2^+-implanted poly-Si source.

Conclusions

The distribution and the roles of fluorine in the BF_2^+-implanted poly-Si/Si have been analyzed in the temperature range from 850 to 1100°C. After thermal annealing, it was observed that a fluorine peak remains in the as-implanted peak regions and a fluorine peak develops at the original poly-Si/Si interface. The fluorine peak in the as-implanted peak regions becomes narrower and lower as annealing temperature increased owing to the outdiffusion of fluorine atoms, except in the 900°C annealed sample. This is ex-

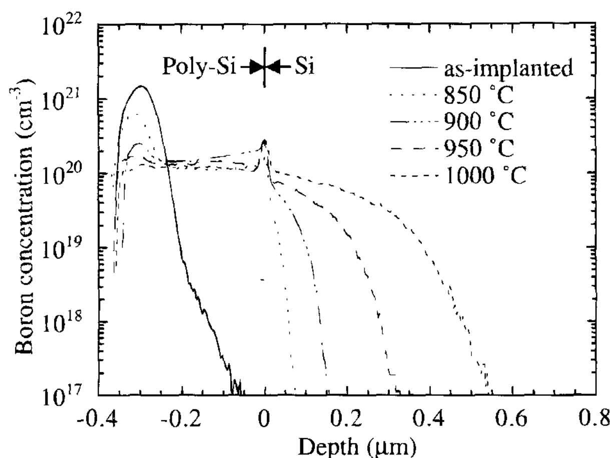

Fig. 9. SIMS boron distribution profiles of BF_2^+ as-implanted poly-Si/Si and thermal annealing at 850, 900, 950, and 1000°C for 30 min.

Downloaded on 2014-04-28 to IP 140.113.38.11 address. Redistribution subject to ECS terms of use (see ecsdl.org/site/terms_use) unless CC License in place (see abstract).

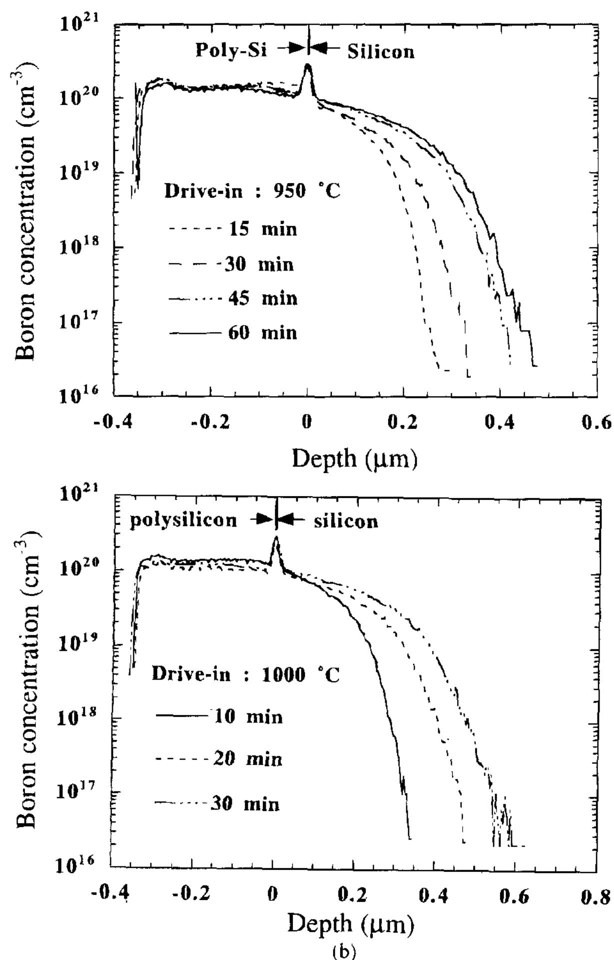

Fig. 10. SIMS boron distribution profiles of BF_2^+ implanted poly-Si/Si after thermal annealing at (a, top) 950 and (b, bottom) 1000°C for 15 to 60 min.

plained by the effects of the outdiffusion of fluorine atoms and the formation of fluorine bubbles. The pileup of fluorine atoms at the poly-Si/Si has the effects of enhancing epitaxial regrowth of poly-Si films and the formation of fluorine bubbles. The formation of fluorine bubbles resulted from the accumulation of fluorine atoms. It was also found that the shapes, the size, and the density of bubbles at the poly-Si/Si interface are related to annealing temperature and time. The appearance of the boron peak at the original poly-Si/Si interface is attributed to be the gettering of boron atoms by the fluorine bubbles. In addition, the presence of fluorine atoms leads to the higher C_s values, and the boron profiles in the silicon substrate are sensitive to thermal budget. The results demonstrated that the presence of fluorine atoms plays an important role in the annealing behaviors of BF_2^+-implanted poly-Si/Si systems.

Acknowledgment

The authors are grateful to C. C. Wang for SIMS measurement. This work was supported by the National Science Council of the Republic of China under Contract No. NSC 84-2215-E009-023.

Manuscript submitted Oct. 7, 1994; revised manuscript received Feb. 16, 1995.

National Chiao Tung University assisted in meeting the publication costs of this article.

REFERENCES

1. M. H. El-Diwany, M. P. Brassington, P. Tuntasood, R. R. Razouk, and M. W. Poulyer, *IEEE Trans. Electron Devices,* **ED-35,** 1556 (1988).
2. G. L. Patton, J. C. Bravman, and J. D. Plummer, *ibid.,* **ED-33,** 1754 (1986).
3. T. Kamins, *Polycrystalline Silicon for Integrated Circuit Applications,* Kluwer Academic, Boston (1988).
4. *Polysilicon Emitter Bipolar Transistors,* A. K. Kapoor and D. J. Roulston, Editors, IEEE Press, New York (1989).
5. J. M. C. Stork, M. Arienzo, and C. Y. Wong, *IEEE Trans. Electron Devices,* **ED-32,** 1766 (1985).
6. K. L. Mclaughlin, M. A. Taylor, and G. Sweeney, *Appl. Phys. Lett.,* **47,** 992 (1985).
7. K. Park, S. Batra, S. Banerjee, G. Lux, and R. Manukondo, *This Journal,* **138,** 545 (1991).
8. I. R. C. Post and P. Ashburn, *IEEE Trans. Electron Devices,* **ED-38,** 2442 (1991).
9. P.-F. Lu, J. D. Warnock, J. D. Cressler, K. A. Jenkins, and K.-Y. Toh, *ibid.,* **ED-38,** 1410 (1991).
10. S. L. Wu, C. L. Lee, T. F. Lei, and H.-C. Chang, *ibid.,* **ED-40,** 1797 (1992).
11. J. J. Sung and C.-Y. Lu, *ibid.,* **ED-37,** 2312 (1990).
12. H.-H. Tseng, M. Orlowski, P. J. Tobin, and R. L. Hance, *IEEE Trans. Electron Device Lett.,* **EDL-13,** 14 (1992).
13. G, D. Williams and P. Ashburn, *J. Appl. Phys.,* **72,** 3169 (1992).
14. S. L. Wu, C. L. Lee, T. F. Lei, C. F. Chen, L. J. Chen, K. Z. Ho, and Y. C. Ling, *IEEE Trans. Electron Device Lett.,* **EDL-15,** 120 (1994).
15. T. P. Chen, T. F. Lei, H. C. Lin, and C. Y. Chang, *This Journal,* **142,** 532 (1995).
16. H. Schaber, R. V. Criegen, and I. Weitiel, *J. Appl. Phys.,* **58,** 4036 (1985).
17. B. Garben, W. A. Orr-Arienzo, and R. L. Lever, *This Journal,* **133,** 2152 (1986).
18. M. Y. Tsai, D. S. Day, B. G. Streetman, P. Williams, and C. A. Evans, *J. Appl. Phys.,* **50,** 188 (1979).
19. C. W. Nieh and L. J. Chen, *Appl. Phys. Lett.,* **48,** 1528 (1986).
20. C. W. Nieh and L. J. Chen, *J. Appl. Phys.,* **60,** 3114 (1986).
21. S.-P. Jeng, T.-P. Ma, R. Canteri, M. Anderle, and G. W. Rubloff, *Appl. Phys. Lett.,* **61,** 1310 (1992).
22. B. Yu, E. Arai, Y. Nishioka, Y. Ohji, S. Iwata, and T. P. Ma, *ibid.,* **56,** 1430 (1990).
23. R.-D. Chang, T.-F. Chen, and J. S. Fu, *SSDM,* 401 (1992).

Downloaded on 2014-04-28 to IP 140.113.38.11 address. Redistribution subject to ECS terms of use (see ecsdl.org/site/terms_use) unless CC License in place (see abstract).